

## Amine Induced Retardation of the Radical-Mediated Thiol-Ene Reaction via the Formation of Metastable Disulfide Radical Anions

Dillon Marshall Love, Kangmin Kim, John Taylor Goodrich, Benjamin D. Fairbanks, Brady T. Worrell, Mark P. Stoykovich, Charles B. Musgrave, and Christopher N. Bowman

*J. Org. Chem.*, **Just Accepted Manuscript** • DOI: 10.1021/acs.joc.8b00143 • Publication Date (Web): 01 Feb 2018

Downloaded from <http://pubs.acs.org> on February 2, 2018

### Just Accepted

“Just Accepted” manuscripts have been peer-reviewed and accepted for publication. They are posted online prior to technical editing, formatting for publication and author proofing. The American Chemical Society provides “Just Accepted” as a free service to the research community to expedite the dissemination of scientific material as soon as possible after acceptance. “Just Accepted” manuscripts appear in full in PDF format accompanied by an HTML abstract. “Just Accepted” manuscripts have been fully peer reviewed, but should not be considered the official version of record. They are accessible to all readers and citable by the Digital Object Identifier (DOI®). “Just Accepted” is an optional service offered to authors. Therefore, the “Just Accepted” Web site may not include all articles that will be published in the journal. After a manuscript is technically edited and formatted, it will be removed from the “Just Accepted” Web site and published as an ASAP article. Note that technical editing may introduce minor changes to the manuscript text and/or graphics which could affect content, and all legal disclaimers and ethical guidelines that apply to the journal pertain. ACS cannot be held responsible for errors or consequences arising from the use of information contained in these “Just Accepted” manuscripts.



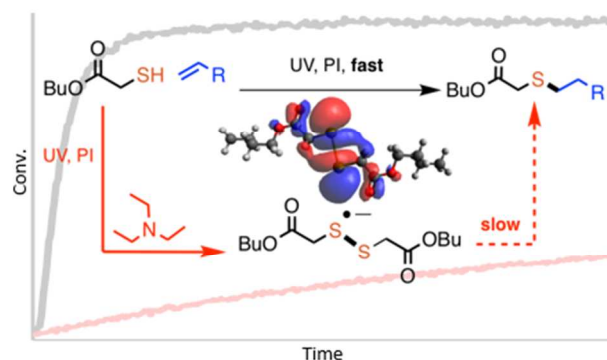
# Amine Induced Retardation of the Radical-Mediated Thiol-Ene Reaction *via* the Formation of Metastable Disulfide Radical Anions

Dillon M. Love,<sup>†</sup> Kangmin Kim,<sup>‡</sup> John T. Goodrich,<sup>†</sup> Benjamin D. Fairbanks,<sup>†</sup> Brady T. Worrell,<sup>†</sup> Mark P. Stoykovich,<sup>||</sup> Charles B. Musgrave,<sup>†,‡,§</sup> and Christopher N. Bowman<sup>\*,†,‡,§</sup>

<sup>†</sup>Department of Chemical and Biological Engineering, <sup>‡</sup>Department of Chemistry and Biochemistry, and <sup>§</sup>Materials Science and Engineering Program, University of Colorado Boulder, Boulder, Colorado 80309, United States

<sup>||</sup> Current Address: The Institute for Molecular Engineering, The University of Chicago, Chicago Illinois, 60637, United States

\*christopher.bowman@colorado.edu



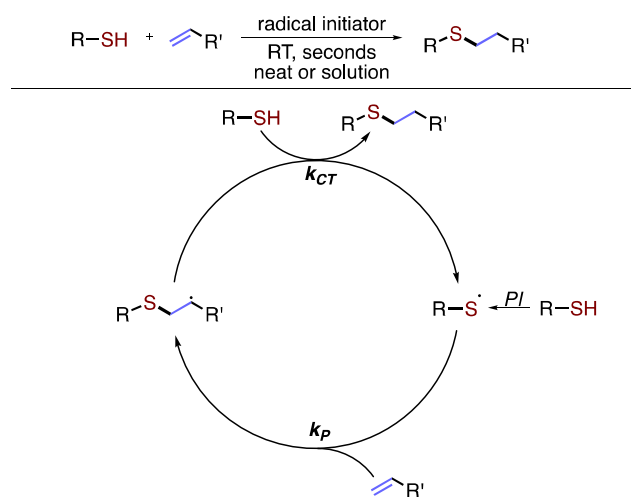
**Abstract:** The effect of amines on the kinetics and efficacy of radical-mediated thiol-ene coupling (TEC) reactions was investigated. By varying the thiol reactant and amine additive, it was shown that amines retard thiol radical-mediated reactions when the amine is adequately basic enough to deprotonate the thiol affording the thiolate anion. E.g. when the weakly basic amine tetramethylethylenediamine was incorporated in the TEC reaction between butyl 2-mercaptoacetate and an allyl ether at 5 mol%, the final conversion was reduced from quantitative to < 40%. Alternatively, no effect is observed when the less acidic thiol butyl 3-mercaptopropionate is employed. The thiolate anion was established as the retarding species through the introduction of ammonium and thiolate salt additives into TEC formulations. The formation of a two-sulfur three-electron bonded disulfide radical anion (DRA) species by the reaction of a thiol radical with a thiolate anion was determined as the cause for the reduction in catalytic radicals and the TEC rate. Thermodynamic and kinetic trends in DRA formations were computed using density functional theory and by modeling the reaction as an associative electron transfer process. These trends correlate well with the experimental retardation trends of various thiolate anions in TEC reactions.

## INTRODUCTION

Thiyl radical chemistry is of exceptional interest in biochemistry<sup>1</sup> and synthetic organic chemistry<sup>2</sup> owing to the ubiquity of thiol containing moieties found in nature and the availability of a diverse range of alkyl and aryl thiols with similar reactive character. Valuable reactions include thiyl radical reactions with thioketones, used in the development of self-healing, thiuram disulfide materials,<sup>3</sup> and reactions with alkynes, or thiol-yne click reaction, which affords two thioether linkages and is a tool of great use in synthesizing materials with complex/branching architectures and in bioconjugation chemistry.<sup>4</sup> Reactions with alkenes, i.e., radical-mediated thiol-ene coupling (TEC) reactions, constitute the most popular and robust thiyl radical transformation, with TEC reactions having become a staple in material fabrication, conjugation chemistry, and to a lesser extent, small molecule synthesis.<sup>5</sup>

Under appropriate implementation conditions, TEC reactions for polymer synthesis and functionalization have been designated as “click” reactions due to their high chemical- and regioselectivity, rapid kinetics, ability to be conducted without solvent, full atom economy, and insensitivity to water and oxygen. The reaction proceeds *via* the cyclic mechanism shown in **Scheme 1**, where the thiyl radical is usually generated using a photoinitiator (P.I.). The thiyl radical then propagates ( $k_p$ ) into the alkene generating a C-S bond and simultaneously forming an intermediate 2° C-radical. The C-radical then chain-transfers ( $k_{CT}$ ) to a thiol *via* H-atom abstraction to regenerate the thiyl radical, resulting in a thioether linkage.

### Scheme 1. TEC Reaction Mechanism



Because TEC reactions do not require toxic metal catalysts and are generally orthogonal to many organic functional group chemistries, they have become a powerful tool in bioconjugation strategies<sup>5a,5e,6</sup> as well as in the formation and modification of cell-encapsulating hydrogels.<sup>7</sup> Further, the orthogonality of TEC reactions allows them to be employed sequentially with thiolate anion ( $\text{RS}^-$ ) mediated addition reactions, which include thioester exchange, thiol-epoxy, thiol-

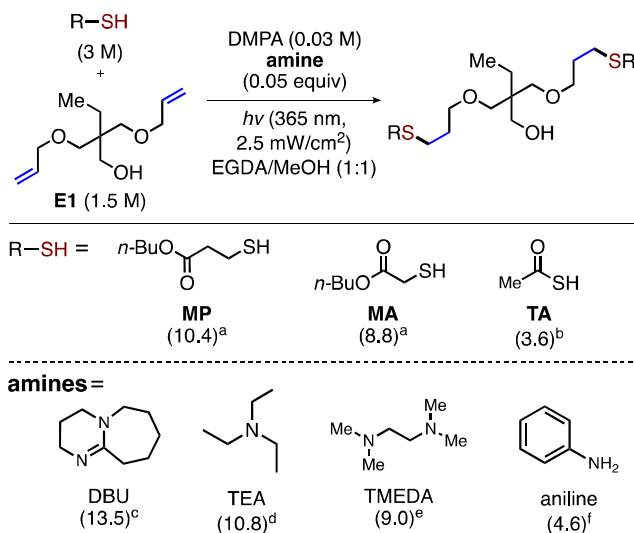
1  
2  
3 isocyanate, and thiol-Michael (base or nucleophile catalyzed) reactions, to synthesize architectures and microstructures of  
4 increasing complexity.<sup>5c,8</sup>

6  
7 Recently, the “click” designation for TEC reactions has been called into question under certain conditions where TEC  
8 reactions do not achieve quantitative conversion without any appreciable side-product formation. For example, recent work in our  
9 lab aimed towards synthesizing nucleobase containing, sequence-ordered polymers with sequential TEC/thiol-Michael reactions  
10 revealed that performing TEC polymerizations in the presence of basic amine functionalities often result in extremely low rates  
11 and poor conversions < 50%, despite the basicity of such groups being too low to induce significant deprotonation of the reactive  
12 thiol groups.<sup>8f</sup> In other recent work, Colack *et al.* investigated the factors that affect thiol-ene kinetics in aqueous environments to  
13 show that thiol conversions drop significantly when the system pH approaches and surpasses the reacting thiol pKa, attributed to  
14 the loss of the thiol group’s ability to react, or when an amine containing buffer is used, for which no mechanism was proposed.<sup>9</sup>  
15 Such results limit the application of TECs in the fabrication of materials possessing complex combinations of functional group  
16 chemistries (e.g. peptides, proteins, nucleic acids, biomimetic materials) or in applications employing consecutive reactions  
17 involving TEC and a reaction with a basic/amine catalyst (e.g. thiol-Michael, thiol-epoxy, thiol-halide, thiol-isocyanate).  
18 Considering these observations, the phenomena that causes the poor performance of the radical-mediated thiol-ene reaction needs  
19 to be better understood for this chemistry to be employed to its fullest potential.

20  
21  
22  
23  
24  
25  
26  
27  
28  
29  
30 In this work, the mechanism by which amines retard radical-mediated TEC reactions within a many-component organic  
31 system, conditions analogous to typical thiol-ene photopolymerizations, was investigated. The results presented establish  
32 guidelines for designing TEC systems and other thiyl radical-mediated transformations by furthering the understanding of the  
33 behavior of S-centered radicals in the context of general synthetic chemistry. Using real-time Fourier transform IR (rt-FTIR)  
34 spectroscopy to monitor the kinetics and long-range hybrid DFT calculations to assess the validity of proposed mechanisms from  
35 both a thermodynamic and kinetic stand point, it was concluded that retardation occurs due to the generation of thiolate anions  
36  $RS^-$  *in situ* by amine facilitated deprotonation. Thiolate anions then react to form a two-sulfur three-electron (2S-3e) covalent  
37 interaction with thiyl radicals, partitioning the catalytic radical species of the TEC reaction into a metastable disulfide radical  
38 anion species. Strong correlations between the retardation activity of various thiolate species and the calculated  $\sigma$ -withdrawing  
39 character of the substituent(s) were observed. Further, when the formation reaction of the disulfide radical anion was modeled as  
40 the reverse of a step-wise dissociate electron transfer (DET) reaction, an inverse correlation emerged between the calculated  
41 magnitude of solvent reorganization required in going from reactants to the transition state and the retardation activity of the  
42 thiolate anion. It was also observed, by selecting TEC systems with rapid kinetics and are not propagation limited (e.g. the  
43 reaction between butyl 3-mercaptopropionate and 5-norbornene-2-methanol), that the retardative effects of the thiolate anion may  
44 be mitigated.

## RESULTS and DISCUSSION

## Scheme 2. TEC Reactions in the Presence of Amines



pKa values for thiols and conjugate acid pKa values for amines shown in parenthesis. Values obtained from references

<sup>a</sup>10, <sup>b</sup>11, <sup>c</sup>12, <sup>d</sup>13, <sup>e</sup>14, <sup>f</sup>15.

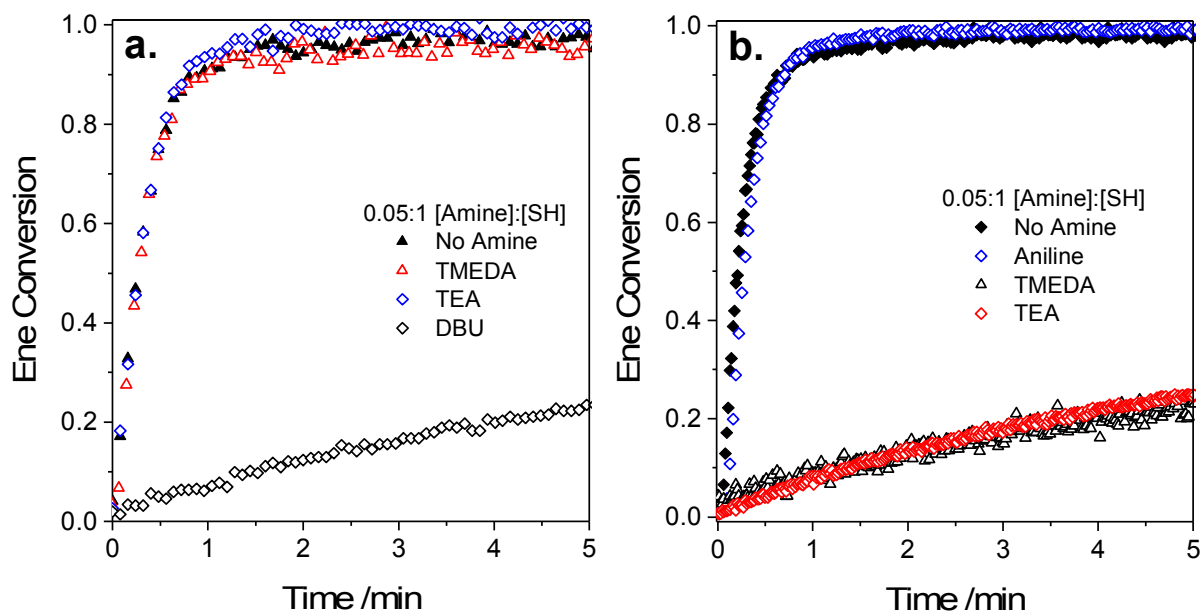


**Figure 1.** Ene conversion versus time for the TEC reaction between (a) **MP** and **E1** (1:1 [SH]:[C=C]), for clarity not all data points are included, and (b) **MA** and **E1** (1:1 [SH]:[C=C]) in the presence of amines with varying basicity. The reactions were formulated with **MP/MA** (3M), **E1** (1.5 M), **DMPA** (0.03 M) with no amine, **TMEDA**, **TEA**, or **DBU** at 5 mol%.

**Amine Effects on the TEC Reaction.** Initially, TEC reactions between several thiols (3 M) and a diallyl ether (**E1**, 1.5 M) (**Scheme 2**) were conducted in the presence of amines of differing basicity, and their kinetics were monitored *via* FTIR when initiated by continuous irradiation with 0.03 M photoinitiator (2,2-dimethoxy-2-phenylacetophenone, DMPA). With 5 mol% amine, the least acidic thiol, butyl 3-mercaptopropionate (**MP**) exhibited retarded kinetics with the strongly basic 1-8-diazabicyclo[5.4.0]undec-7-ene, DBU, while remaining unaffected by the less basic triethylamine, TEA, and tetramethylethylenediamine, TMEDA (**Figure 1A**). The more acidic thiols butyl 2-mercaptoacetate (**MA**, see **Figure 1B**) and thioacetic acid (**TA**, **Figure S2**) were retarded in the presence of DBU, TEA, and TMEDA, with the most acid thiol, **TA**, being the only thiol retarded by the least basic amine, aniline. In all cases, reactions exhibited reduced rates and conversions only when the aqueous pKa of the thiol was lower than the conjugate acid pKa of the amine additive, indicating that the thiol must be deprotonated by the amine for the system to exhibit retardation (i.e. the  $RS^-$  or ammonium ion must be present).

The retardation activity,  $R_0/R$ , defined here as the ratio of the steady-state reaction rate for the TEC reaction in the absence ( $R_0$ ) relative to in the presence of an additive ( $R$ ), of DBU in the **MP/E1** reaction was characterized. With 1, 2.5, 5, and 25 mol% DBU,  $R_0/R$  values of 1.1, 9.9, 43, and 180 were obtained, respectively. The 1 mol% DBU sample achieved 100% conversion after 2 min irradiation, while the 2.5 mol% sample reduced the rate by a factor of  $\sim 10$  and limited the conversion to  $\sim 30\%$ . 25 mol% DBU effectively prevented any reaction (see **Figure 2**). These results, along with the pKa trend, demonstrate that retardation is a result of either the ammonium or thiolate ion interacting with a TEC radical.

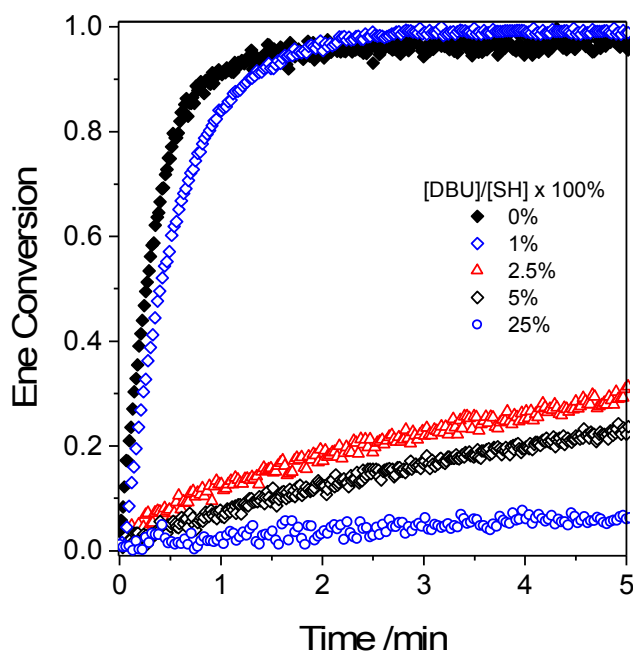


**Figure 2.** Ene conversion versus time for the TEC reaction between MP and E1 (1:1 [SH]:[C=C]) in the presence of 0, 1, 2.5, 5, and 25 mol% DBU.

**Amine Effects on the Thiol-Yne Reaction.** The same retardation trends established with the **E1** TEC reactions were also observed in the radical-mediated thiol-yne reaction (**Table 1**) between **MP** or **MA** with the alkyne 4-octynyl-1-ol (**Y1**) (see **Scheme S1**). Thiol-yne reactions are similar to TEC reactions; the thiyl radical propagates into the alkyne generating a vinyl sulfide functionality, followed by a more rapid second thiyl radical addition<sup>16</sup> affording a dithioether product. The **MP/Y1** reaction (**Figure S4**) exhibited limited final conversions when 1 mol% DBU was present (66% yne conversion) while TEA and TMEDA had a minimal effect on the rate and no effect on conversion. The **MA/Y1** reaction (**Figure S5**) was significantly retarded when DBU, TEA, or TMEDA were present at 1 mol% and relatively unaffected by aniline at 25 mol%, as expected. These results allow for the rule for amine retardation of TEC reactions (that retardation occurs when the amine is basic enough to deprotonated the thiol reactant) to be extended to thiyl radical reactions, in general. Interestingly, the retardation activities increased by at least an order of magnitude for this thiol-yne reaction versus the TEC reactions with **E1**, e.g.  $R_0/R = 1.12$  and 16 for **MP/E1** and **MP/Y1**, respectively, with 1 mol% DBU present, and  $R_0/R = 1.8$  and 40 for **MA/E1** and **MA/Y1**, respectively, with 1 mol% TMEDA present. Previous work in the Bowman Lab focusing on thiol-yne kinetics had found the alkyne, methyl propargylamine, to exhibit limited conversions and slow kinetics in lieu of its electron rich character.<sup>16b</sup> The results presented here demonstrate that the observed phenomena was a result of the basic character of the alkyne functionality being investigated rather than the reactive character of the propargyl amine functional group towards thiyl radicals.

**Table 1. Effect of Amines on the Thiol-Yne Reaction**

Thiol	Additive	Equiv	$R_0/R^a$	Alkyne Conversion (%) <sup>b</sup>
MP	--	--	1	quant.
MP	DBU	0.01	12(±6)	66(±11)
MP	DBU	0.05	7400(±1200)	25(±2)
MP	TEA	0.25	1.5(±0.3)	quant.
MP	TMEDA	0.25	1.6(±0.2)	quant.
MA	--	--	1	quant.
MA	DBU	0.01	13000(±2000)	16(±2)
MA	TEA	0.01	20(±2)	67(±2)
MA	TMEDA	0.01	40(±10)	60(±10)
MA	TMEDA	0.05	18000(±3000)	12(±2)
MA	Aniline	0.25	1.8(±0.2)	quant.

Thiol-yne reaction between **MP** or **MA** and **Y1**, 2:1 [SH]:[Yne], formulated with amine additives.<sup>a</sup> The steady-state propagation rate  $R_0 = 9.3$  and  $10.8 \text{ M min}^{-1}$  for **MP** and **MA**, respectively, with **Y1** when no additive is present.<sup>b</sup> Conversions determined by FTIR *in situ* from the decrease in the C–H peak corresponding to the alkyne functional group at  $3330 \text{ cm}^{-1}$ . Conversions correspond to 10 min of irradiation.

## Scheme 3. TEC Reactions in the Presence of Ammonium and Thiolate Salts

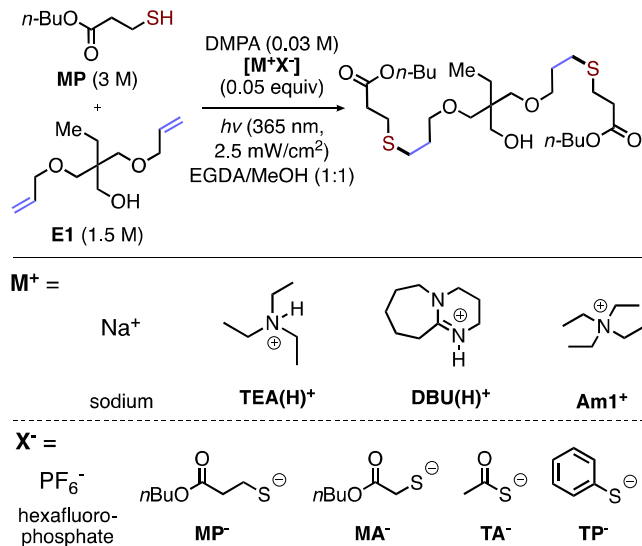


Table 2. Effects of Ammonium and Thiolate Ions on TEC

Additive (0.05 equiv)			$R_0/R$ <sup>a</sup>	Ene conversion (%) <sup>b</sup>
Anion	Cation	Amine		
		DBU	44(±3)	35(±6)
		TEA	1.0(±0.1)	quant.
$\text{AcO}^-$	$\text{TEA(H)}^+$		0.82(±0.04)	quant.
	$\text{DBU(H)}^+$		1.09(±0.06)	quant.
$\text{PF}_6^-$	$\text{Am1}^+$		1.4(±0.2)	quant.
$\text{MP}^-$	$\text{Na}^+$		3.4(±0.7)	quant.
	$\text{Am1}^+$		6(±1)	92(±4)
$\text{TP}^-$	$\text{Na}^+$		49(±22)	45(±2)
	$\text{Am1}^+$		41(±12)	49(±5)
$\text{TA}^-$	$\text{Na}^+$		3.3(±0.4)	quant.
	$\text{Am1}^+$		2.6(±0.7)	quant.
$\text{MA}^-$	$\text{Na}^+$		125(±64)	21(±5)
	$\text{Am1}^+$		140(±80)	16(±8)

TEC reaction between **MP** and **E1**, 1:1 [SH]:[C=C], formulated with amine or salt additives, 0.05:1 [additive]:[SH]. <sup>a</sup>  $R_0=5.65 \text{ M min}^{-1}$  <sup>b</sup> Conversions determined by FTIR *in situ* from the decrease in the C–H peak corresponding to the alkene functional group at  $3050 \text{ cm}^{-1}$ . Conversions correspond to 10 min of irradiation.

**Effect of Ammonium and Thiolate Ions on TEC Reactions.** Effects of ammonium cations, quaternary and protonated tertiary amines, and thiolate anions on the **MP/E1** reaction were studied by introducing 5 mol% salt additives

(Scheme 3). The salts of protonated TEA and DBU with acetate,  $[\text{TEA}(\text{H})^+ \text{AcO}^-]$  and  $[\text{DBU}(\text{H})^+ \text{AcO}^-]$ , show no effect on the reaction rate (Table 2); likewise, similar rates were observed with the quaternary ammonium containing salt  $[\text{Am1}^+ \text{PF}_6^-]$ . For all formulations without thiolate anions present, quantitative conversions by FTIR were achieved in  $\sim 2$  min irradiation, ruling out the potential of radical chain-transfer to protonated amine or other radical side-reactions with amine additives employed in the previous section. Figure S6 compares the impact of the anion on MP/E1 while keeping the cations structure constant, i.e.,  $\text{Am1}^+$ . The anion  $\text{PF}_6^-$ , exhibits slightly delayed kinetics, with the rates shown in Table 2, but quantitative conversion continues to be achieved around  $\sim 2$  min irradiation.

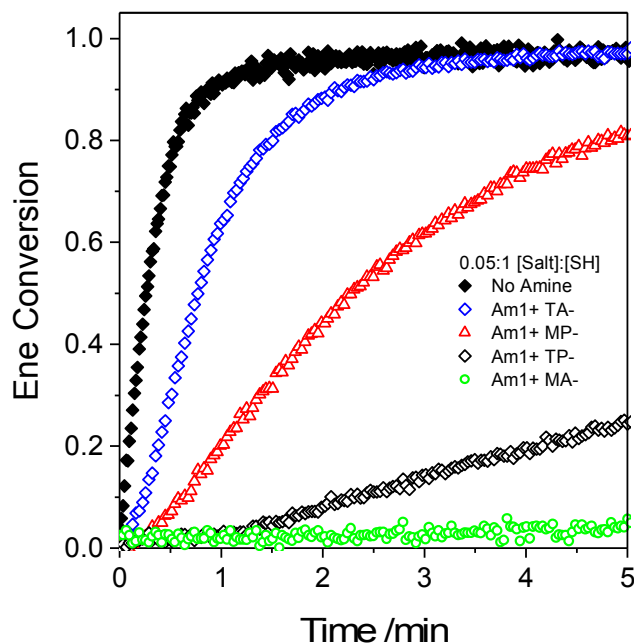


**Figure 3.** Ene conversion versus time for the TEC reaction between **MP** and **E1** (1:1 [SH]:[C=C]) in the presence of salt additives. The reaction samples were formulated with with no salt,  $[\text{Am1}^+ \text{TA}^-]$ ,  $[\text{Am1}^+ \text{MP}^-]$ ,  $[\text{Am1}^+ \text{TP}^-]$ , and  $[\text{Am1}^+ \text{MA}^-]$ .

The  $\text{MP}^-$  anion resulted in significantly suppressed reaction rates,  $R_0/R = 6$ , and a delayed time to completion,  $> 5$  min irradiation. Given that for **MP/E1** reactions at steady-state it is expected that  $R \propto [\text{C}\cdot]$ ,<sup>17</sup> where  $[\text{C}\cdot]$  is the concentration of  $2^\circ$  C-radicals, the steady-state reaction rates for **MP/E1** with  $[\text{Am1}^+ \text{PF}_6^-]$  and  $[\text{Am1}^+ \text{MP}^-]$  correspond to approximately an 18% and 71% reduction in  $[\text{C}\cdot]$ , respectively. Figure 3 compares the results of varying the thiolate anion structure while keeping the cation structure constant as  $\text{Am1}^+$ , where the thiolate retardation activities follow the trend:  $\text{MA}^- > \text{TP}^- > \text{MP}^- > \text{TA}^-$ , with the  $\text{MA}^-$  anion effectively preventing any significant reaction from occurring as an average ene conversion of 19% was obtained with the  $\text{MA}^-$  with two counterions. Retardation activity trends persist independent of the counter ion structure ( $\text{Na}^+$  or



radicals. TEC reactions between **MP** and three alkenes (**E1**, 5-norbornene-2-methanol **E2**, and 1,3-divinyltetramethyldisiloxane **E3**) were conducted with 5 mol% DBU or  $RS^-$  salt (**Scheme 4**).  $k_p/k_{CT}$  for **MP/E1** and **MP/E2** was previously determined to be  $\sim 10$  and  $\sim 1$ ,<sup>17</sup> respectively, while for the **MP/E3** reaction  $k_p/k_{CT} = 0.2$  (See **SI Section 6**).  $R_0/R$  values and final ene conversions are in **Table 3**.  $R_0/R$  trends correlate with  $k_p/k_{CT}$ , i.e. the higher ratio of thiyl radicals to C-radicals is, the more retarded the system is by amine and  $RS^-$  additives.  $[Am1^+ MP^-]$  reduced the rates for the **MP/E1**, **MP/E2**, and **MP/E3** systems to 18 %, 2 %, and 0.3 % of the control rates, respectively, and  $[Am1^+ TP^-]$  reduced the rates to 2 %, 1 %, and 0.07 %, respectively. Comparing the chain-transfer limited **MP/E1** and the propagation limited **MP/E3**, which should decrease the  $[C\cdot]/[S\cdot]$  ratio, the average  $R_0/R$  values of the three additives increase by a factor of  $\sim 30$  for DBU and  $TP^-$  and a factor of  $\sim 60$  for  $MP^-$ . This correlation indicates that retardation is the result of a thiolate-thiyl radical interaction. Owing to the rapid kinetics of the thiol-norbornene reactions, **MP/E2** systems still reached quantitative conversions in each formulation prior to 10 min irradiation, implying that thoughtful selection of the alkene functionality at least somewhat mitigates the impact of the thiolate/amine induced retardation effects on conversion in thiol-ene systems.

It should be noted that retardation persisted when the TEC reactions were initiated *via* direct irradiation without photoinitiator (**SI Section 7**), ruling out the potential of a thiolate-initiator interaction as the retardation mechanism.

**Computational Investigation of the Thiyl Radical-Thiolate Anion Interaction.** Formation of a 2S-3e bonded metastable disulfide radical anion (DRA) by association of a thiyl radical with a thiolate ion ( $RS\cdot + R'S^- \leftrightarrow [RSSR']^-$ ) was hypothesized as the cause of the retardation. DRAs occur as intermediates in biochemical processes, e.g. metabolism and disulfide bridge exchange,<sup>19</sup> primarily studied under physiologically relevant environments.<sup>20</sup> Further, hitherto performed DRA studies on thermodynamic stability, and formation/fragmentation kinetics describe reactions of biochemically relevant thiols without consideration towards moieties frequently employed in TEC formulations, namely mercaptopropionate, mercaptoacetate, and thioacetate. Given the deficit in the literature regarding DRA formations in non-physiological environments, especially in relatively nonpolar and viscous organic environments, and the limited diversity of published DRA structures, DFT calculations were performed to explore the thermodynamics and kinetics of DRAs in the context of TEC reactions.

DRA formations from the various parent thiols used in this study were thermodynamically favorable in a modeled solvent environment due to the enhanced charge delocalization in the DRAs vs. the thiolate anions and a favorable enthalpic contribution from the S-S bond formation.<sup>20a,20b</sup> The **MPMA** DRA was found to be the most stable and the **MPTA** DRA, the least stable (-17.9 vs. -6.4 kcal/mol) while other DRAs have intermediate stabilities (**Table 4**). The behavior of the computationally calculated stabilities agrees well with the experimental trends where the **MPMA** formulation exhibited two orders of magnitude greater retardation compared to that of **MPTA** while other DRAs induced intermediate degrees of retardation. It is expected that the differences in the degrees of retardation between formulations originate from the environment

of the radical electron density in each DRA. The population analysis of the radical density on the disulfide bond ( $\rho[\sigma_{SS}^*]$ ) demonstrates that the ester groups in **MA** and **MP**, and to a lesser degree, the phenyl group in **TP** withdraws electron density from the antibonding  $\sigma_{SS}^*$  orbital, increasing the stability of the DRAs. In contrast, the acetyl group of **TA** donates electron density to the  $\sigma_{SS}^*$  orbital, decreasing the stability of the associated DRA.<sup>21</sup> (**Table 4**) This behavior is due to the mismatch in size between the 3p atomic orbital (AO) of sulfur and 2p AO of carbon<sup>22</sup> that limits the electronic delocalization through the  $\pi$ -system and ultimately results in the pronounced effect of the inductive electron-withdrawing character (EWC) in substituents.<sup>23</sup> Asymmetric DRAs exhibit EWC averaged over the two substituents. Also important are the results from an analysis of the difference of the localized electronic densities on each S-nucleus of the DRAs ( $\rho$  *diff.*), which reveals an additional cause for the instability of **TA**-derived DRAs. (**Table 4**) When the two sulfur nuclei possess equivalent electronic states or nearly so, an additional degeneracy is introduced that stabilizes the DRA via resonance between the two sulfur fragments.<sup>24</sup> All symmetric DRAs except for **TATA** exhibited minimal electron density differences between the anionic and radical S-nuclei whereas the radical S-nucleus had a more localized density than the anionic S-nucleus in **TATA**.<sup>24a</sup> Among asymmetric DRAs, **MPTA** again exhibited the largest electron density difference, leading to its thermodynamic instability. This result is accompanied by a highly correlated linear relationship between  $\Delta G^\circ$  and  $\rho$  *diff.* ( $R^2 = 0.92$ ), excepting **MPMA** (**Figure 4a**). The exceptional stability of **MPMA** is attributed to negative hyperconjugation resulting from the syn-periplanar position of the  $\pi_{C=O}$  and  $\sigma_{C-S}^*$  orbitals in the **MA** substituent (**Figure 4b**).<sup>25</sup> This additional stabilizing electronic effect results in the lengthening of the C–S and C=O bonds as electron density from the  $\pi_{C=O}$  bonding orbital transfers to the  $\sigma_{C-S}^*$  antibonding orbital. The required orbital overlap for hyperconjugation was not predicted for any other DRAs including **MAMA**. Therefore, it was concluded that the degree of inductive EWC and the balance of the electron density distribution between the two S-nuclei are the principal reasons for the experimental trend.

**Table 4. Computational Data on the Formulation of Disulfide Radical Anions**

DRA	$\Delta G^\circ$	K	$\rho[\sigma_{SS}^*]$	BDE <sup>a</sup>	$\lambda_{total}$	$\Delta G^\ddagger$
TPTP	-14.0	1.8E+10	-0.94	59.4	1.4	9.0
TATA	-11.2	1.8E+08	-1.21	55.4	5.6	10.1
MAMA	-13.7	1.0E+10	-0.66	59.5	3.6	9.7
MPMP	-15.0	1.0E+11	-0.90	60.7	3.1	9.3
MPTP	-8.8	2.8E+06	-0.95	58.3	1.5	10.9
MPTA	-6.4	4.7E+04	-1.07	57.4	3.3	12.2
MPMA	-17.9	1.3E+13	-0.90	63.9	2.7	8.9

<sup>a</sup> Bond dissociation energies of corresponding neutral disulfide molecules. Values for  $\Delta G^\circ$ , BDE,  $\lambda_{total}$ , and  $\Delta G^\ddagger$  are in kcal mol<sup>-1</sup>

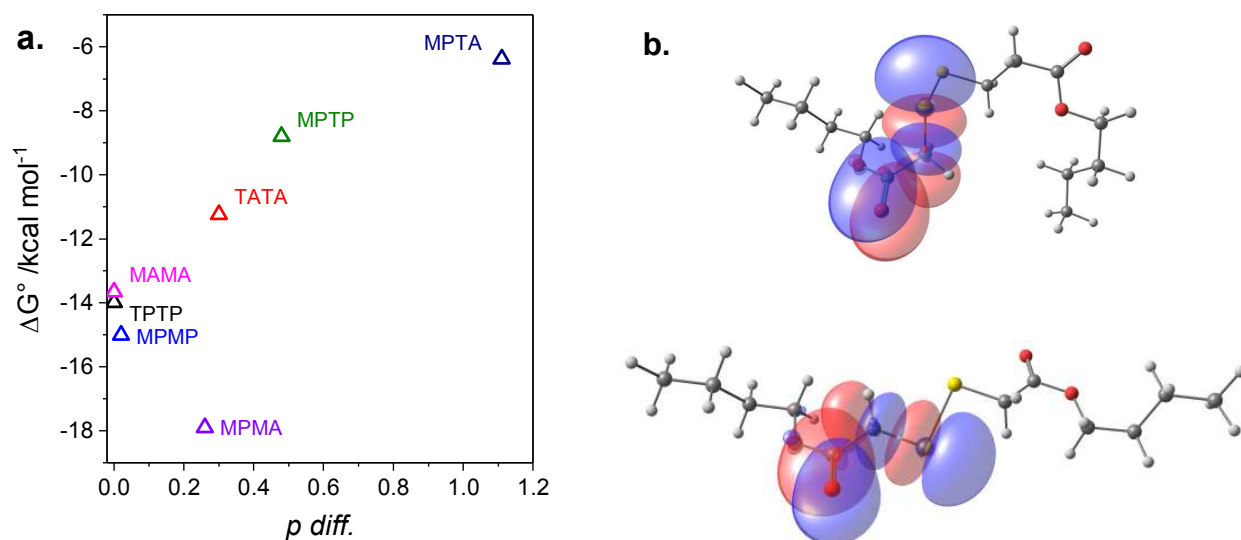


**Figure 4.** (a) Correlation of DRA stability  $\Delta G^\circ$  with the difference of the localized electronic densities on each S-nucleus of the DRAs ( $\rho$  diff.). The **MPMA** DRA is an anomaly due to its unique electronic configuration. (b) Comparison of the  $\pi_{C=O}$  and  $\sigma_{C-S}^*$  orbitals in the (upper) **MPMA** and (lower) **MAMA** radical anions. The unique syn-periplanar positioning of these orbitals in **MPMA** results in a stabilizing orbital overlap.

Saveant's model of dissociative electron transfer (DET) was applied to study the kinetics of DRA formations and specifically, how  $\Delta G^\circ$ , BDE, and  $\lambda_{\text{total}}$  contribute to the activation free energy ( $\Delta G^\ddagger$ )<sup>26</sup> for the ET reaction. This DET theory models an ET reaction that is concomitant with a bond dissociation, in this case through a radical anion intermediate. The reverse reaction --- associative ET --- is analogous to the hypothesized mechanism for DRA formation. Again, the calculations demonstrated that **MPMA** has the smallest activation barrier and **MPTA**, the largest (8.9 vs. 12.2 kcal/mol) with other DRA formations possessing intermediate barriers, further corroborating the agreement between the computational and experimental results. However, neither the stability nor the barrier studies explain why **MPTP** display a higher retardation rate than **MPMP**. Kinetic calculations affirm that **MPTP**'s anomalous retardation activity results from the unusual behavior of the reorganization energy in low polar and viscous resin environments. The rigidity of aromatic structures, such as in **TP**, reduces the required changes in structure that occur during the ET reaction, leading to a low internal reorganization energy ( $\lambda_i$ ).<sup>27</sup> **MA** in the **MPMA** DRA may also experience a similar rigidity effect due to the partial double bond character that arises from hyperconjugation. In contrast, **TA** undergoes significant changes in its bond lengths, bond angles and dihedral angle torsions upon ET, requiring a large  $\lambda_i$ . (See **SI Section 9** for a comparison of the geometric relaxations of **TP** and **TA** upon ET) In low polarity environments, low  $\lambda_i$  as in **TP** and **MP** likely leads to low solvent reorganization energies ( $\lambda_s$ ) because molecular translation for solvent cavity formation becomes the dominant mode for  $\lambda_s$  rather than a change in dipole orientation resulting from electrostatic interactions of reacting species in conventional polar environments.<sup>28</sup> Furthermore, high viscosity is correlated with longer solvent response times which reduces the population of reacting species in the transition state, effectively rendering the low  $\lambda_s$  requirement more crucial in overcoming

1  
2  
3 the activation barrier.<sup>29</sup> Considering the two factors of low solvent polarity and high solvent viscosity, it is proposed that in the  
4 system under consideration and other similar systems that both reorganization energies contribute more to the barrier for the  
5 associative ET reaction of DRA formation than in standard Saveant DET models where low  $\lambda_i$  leads to low  $\lambda_s$  due to low polarity  
6 solvent and the effect of low  $\lambda_s$  is accentuated by high viscosity solvent. This assumption provides the explanation of the greater  
7 retardation activity of the **TP** thiolate anion over the **MP** anion in the **MP/EI** TEC formulation ( $\lambda_{\text{total}} = 1.5$  vs. 3.1 kcal/mol).  
8  
9

## 12 CONCLUSION

13  
14 In this work, it was determined that amines indirectly retard radical-mediated TEC reactions through the *in situ*  
15 generation of the thiolate anion that sequesters the catalytic radical population into a metastable DRA species. The degree of  
16 retardation increases with the ratio of thiyl to carbon radicals present, thiolate anion concentration, and the stability of the  
17 resulting DRA. DFT calculations showed that DRAs comprised of parent thiol fragments investigated in the experimental  
18 kinetics studies are all thermodynamically favorable to form. As the reaction is highly reversible, the thermodynamics is a  
19 governing parameter to predict the degree of retardation and fits well with the observed retardation activities of the thiolate  
20 anions on MP thiol-ene systems, except for the MPTP DRA as the TP anion exhibited exceptional activity. The energetic barriers  
21 to DRA formation were investigated using parameters from the Savaeant model for DET reactions, treating the formation as an  
22 associative ET reaction. It is expected that, due to the relatively high viscosity and low polarity/dielectric character of the reaction  
23 medium, the solvent reorganization is a more significant parameter to the kinetic barrier than is assumed in standard DET  
24 Saveant models. Accordingly, TP anions were determined to have reduced activation barriers toward DRA formation owing to  
25 the rigidity of the aromatic substituent, explaining their high retardation activity and highlighting that conventional ET theories  
26 may not optimally describe ET reactions in a solvent environment that polymer chemists frequently encounter (e.g. relatively  
27 nonpolar and viscous).  
28  
29  
30  
31  
32  
33  
34  
35  
36  
37  
38

39 These results have important implications for the design of TEC systems, and thiyl radical reactions in general, when it  
40 is desired to perform these reactions under alkaline conditions or in the presence of basic moieties. Although, computations and  
41 experiments showed that the DRAs are in general thermodynamically favorable to form when the thiolate anion is present,  
42 quantitative conversions may still be obtained by appropriate selection of the reacting thiol and alkene substrate, i.e. using a thiol  
43 with low acidity or an alkene, like norbornene or vinyl ether, which has rapid curing kinetics under controlled conditions that are  
44 not propagation limited (e.g. divinyl siloxane), or by incorporation of acids in the reaction mixture. Additionally, amines or  
45 thiolate-containing salts could be used as formulation stabilizers, or used to control formulation curing rates.  
46  
47  
48  
49  
50  
51

## 52 EXPERIMENTAL SECTION

53  
54 **General Experimental Methods.** Thiol-ene reaction rate studies were performed on thiol-ene mixtures in the mid IR  
55 (Nicolet Magna-IR 750 series II FTIR spectrometer). Samples were deposited between two sodium chloride plates separated by a  
56  
57  
58  
59  
60

0.051 mm plastic spacer. Thiol ( $2570\text{ cm}^{-1}$ , S–H stretch) and alkene ( $3050\text{ cm}^{-1}$ , C=C–H stretch) conversions were monitored in real-time at a collection rate of  $\sim 1$  scan per second and a resolution of  $1\text{ cm}^{-1}$ . Samples were irradiated until the reaction was complete, as indicated by the functional group absorption peak no longer decreasing, with UV-light from an Acticure 4000 light source with a 365-nm filter at an intensity of  $2.5\text{ mW cm}^{-2}$ . Irradiation intensities were measured with a NIST Traceable Radiometer Photometer, model IL1400A.

All starting materials were obtained commercially without further purification.  $^1\text{H}$  NMR spectra were recorded on Bruker Avance-III 400 spectrometers.

**Computational Methods.** Quantum calculations describing the disulfide radical anion formation were performed at the LC-*w*PBE/aug-cc-PVTZ//LC-*w*PBE/6-31+G\*\* level of DFT,<sup>30</sup> solvated by the ethyl acetate CPCM<sup>31</sup> continuum solvent model with the GAUSSIAN09 software package.<sup>32</sup> Frequency calculations were performed at the LC-*w*PBE/6-31+G\*\* level of theory to confirm optimized geometries and for thermochemical analysis. Overestimated entropies for the solution-phase reaction were corrected by subtracting the translational entropy contribution ( $-TAS^\circ_{\text{Trans}}$ ) from the free energies of reactants and products in solution.<sup>33</sup> The atomic polar tensor population (ATP) analysis<sup>34</sup> was used to analyze electron density distributions of disulfide radical anions and reorganization energies ( $\lambda$ ) were calculated as described by Cossi and Barone.<sup>35</sup> The B3P86 /6-31G\* level of theory<sup>36</sup> was used to calculate the bond dissociation energies (BDE) of disulfides.<sup>37</sup> See **SI Section 9** for additional computational details.

**Synthesis of protonated tertiary amine/acetate salts.** [*AcO*<sup>-</sup> *TEA(H)*<sup>+</sup>] and [*DBU(H)*<sup>+</sup> *AcO*<sup>-</sup>] were prepared using a modified literature procedure.<sup>38,39</sup> Glacial acetic acid (0.1 mL, 1.75 mmol) was added dropwise into a scintillation flask charged with the appropriate amine (1.66 mmol). The reaction was stirred for 6 h at room temperature. Excess acetic acid and amine was removed under vacuum and the resulting product was left under high vacuum and while being heated ( $50\text{ }^\circ\text{C}$ ) for 48 h.

**Synthesis of sodium thiolate salts.** General Procedure: Mono functional thiol (10 mmol) was added dropwise, under a nitrogen environment, into a scintillation flask charged with sodium hydroxide (390 mg, 9.8 mmol) dissolved in 1 mL of deionized water. The reaction was stirred for 30 minutes at room temperature. Water and excess thiol was removed under vacuum and the solids were triturated with cyclohexane (3x 5 mL), ethyl acetate (2 x 5 mL) and ice cold water (1x 5 mL) to afford the desired salts. The salts were left under vacuum until use to prevent the formation of disulfides.

*Sodium/butyl 3-mercaptopropionate thiolate* [*Na*<sup>+</sup> *MP*<sup>-</sup>]. Salt was obtained as a white solid (1.46 g, 81 % yield).  $^1\text{H}$  NMR (400 MHz, Methanol-*d*4)  $\delta$  4.13 (td, 2H), 2.75 (m, 2H), 2.66 (m, 2H), 1.64 (m, 2H), 1.42 (m, 2H), 0.97 (t, 3H);  $^{13}\text{C}$  NMR (101 MHz, Methanol-*d*4) 172.1, 64.1, 38.2, 30.5, 19.0, 18.8, 12.7.

1  
2  
3 *Sodium/thiophenolate [Na<sup>+</sup> TP]*. Salt was obtained as a white solid (1.10 g, 85 % yield). <sup>1</sup>H NMR (400 MHz,  
4 **Methanol-d4**) δ 7.38 (m, 2H), 6.92 (m, 2H), 6.77 (m, 1H); <sup>13</sup>C NMR (101 MHz, **Methanol-d4**) 147.3, 132.9 (2C), 126.9 (2C),  
5 120.1.  
6  
7

8  
9 *Sodium/thioacetate [Na<sup>+</sup> TA]*. Salt was obtained as a white/yellow solid (700 mg, 73 % yield). <sup>1</sup>H NMR (400 MHz,  
10 **Methanol-d4**) δ 2.43 (s, 3H); <sup>13</sup>C NMR (101 MHz, **Methanol-d4**) 219.1, 37.1.  
11  
12

13 *Sodium/butyl 3-mercaptoacetate thiolate [Na<sup>+</sup> MA]*. Salt was obtained as a white solid (1.02 g, 61 % yield). <sup>1</sup>H NMR  
14 (400 MHz, **Methanol-d4**) δ 4.15 (td, 2H), 3.29 (s, 2H), 1.66 (m, 2H), 1.44 (m, 2H), 0.97 (t, 3H); <sup>13</sup>C NMR (101 MHz,  
15 **Methanol-d4**) 171.6, 65.0, 30.4, 25.4, 18.7, 12.8.  
16  
17

18  
19 **Synthesis of tetraethylammonium/thiolate salts [AmI<sup>+</sup> RS]**. General Procedure: Mono functional thiol (1.75 mmol)  
20 was added dropwise, under a nitrogen environment, into a scintillation flask charged with tetraethylammonium hydroxide (0.927  
21 mL, 1.66 mmol) in methanol. The reaction was stirred for 30 minutes at room temperature. Solvent and excess thiol were  
22 removed under vacuum and the solids were triturated with cyclohexane (3x 5 mL), ethyl acetate (2x 5 mL) and ice cold water (1x  
23 5 mL) to obtain the desired thiolate salt. The salts were then placed under vacuum until use to prevent disulfide formation.  
24  
25  
26  
27

28 *Tetraethylammonium/butyl 3-mercaptopropionate thiolate [AmI<sup>+</sup> MP]*. Salt was obtained as a yellow grease. (250 mg,  
29 52 % yield). <sup>1</sup>H NMR (400 MHz, **Methanol-d4**) δ 4.13 (t, 2H), 3.33 (m, 8H), 2.74 (m, 2H), 2.65 (td, 2H), 1.65 (p, 2H), 1.43 (h,  
30 2H), 1.32 (tt, 12H), 0.97, (t, 3H); <sup>13</sup>C NMR (101 MHz, **Methanol-d4**) 172.2, 64.1, 51.9 (4C), 38.1, 30.4, 18.9, 18.8, 12.6, 6.2  
31 (4C).  
32  
33  
34

35  
36 *Tetraethylammonium/thiophenolate [AmI<sup>+</sup> TP]*. Salt was obtained as a yellow grease. (270 mg, 68 % yield). <sup>1</sup>H NMR  
37 (400 MHz, **Methanol-d4**) δ 7.25(m, 4H), 7.13 (m, 1H), 3.31 (m, 8H), 1.30 (tt, 12H); <sup>13</sup>C NMR (101 MHz, **Methanol-d4**) δ  
38 131.7, 128.7 (2C), 128.4 (2C), 124.7, 51.8 (4C), 6.1 (4C).  
39  
40

41 *Tetraethylammonium/thioacetate [AmI<sup>+</sup> TA]*. Salt was obtained as a yellow grease. (220 mg, 65 % yield). <sup>1</sup>H NMR  
42 (400 MHz, **Methanol-d4**) δ 3.30 (q, 8H), 2.44 (s, 3H), 1.31 (tt, 12H); <sup>13</sup>C NMR (101 MHz, **Methanol-d4**) δ 218.7, 51.9 (4C),  
43 37.1, 6.2 (4C).  
44  
45  
46

47 *Tetraethylammonium/butyl 2-mercaptoacetate thiolate [AmI<sup>+</sup> MA]*. Salt was obtained as light red grease. (210 mg, 45  
48 % yield). <sup>1</sup>H NMR (400 MHz, **Methanol-d4**) δ 4.15 (t, 2H), 3.32 (q, 8H), 1.66 (m, 2H), 1.44 (m, 2H), 1.32 (tt, 12H), 0.97 (t,  
49 3H); <sup>13</sup>C NMR (101 MHz, **Methanol-d4**) δ 171.5, 65.0, 52.1 (4C), 30.4, 25.5, 18.8, 12.8, 6.6 (4C).  
50  
51  
52  
53  
54  
55  
56  
57  
58  
59  
60

## ASSOCIATED CONTENT

### Supporting Information

The Supporting Information is available free of charge on the ACS Publications website.

Supplementary figures, kinetic modeling of the **MP/E3** TEC reaction, detailed computational methods, coordinates for optimized molecular structures (PDF)

## AUTHOR INFORMATION

### Corresponding Author

\* [Christopher.bowman@colorado.edu](mailto:Christopher.bowman@colorado.edu)

### Notes

The authors declare no competing financial interests.

## ACKNOWLEDGMENTS

We gratefully acknowledge financial support from NSF-MRSEC (DMR 1420736), DoEd GAANN program and NSF CHE-1214131. We also gratefully acknowledge use of XSEDE supercomputing resources (NSF ACI-1053575).

## REFERENCES

- (1) (a) Chatgililoglu, C.; Asums, K.-D. *Sulfur-Centered Reactive Intermediates in Chemistry and Biology*, 1st ed.; Plenum Press: New York, 1990. (b) Kalyanaraman, B. *Biochem. Soc. Symp.* **1995**, *61*, 55–63. (c) Nagy, P. *Antioxid. Redox Signal.* **2013**, *18* (13), 1623–1641.
- (2) Dénès, F.; Pichowicz, M.; Povie, G.; Renaud, P. *Chem. Rev.* **2014**, *114*, 2587–2693.
- (3) Amamoto, Y.; Otsuka, H.; Takahara, A.; Matyjaszewski, K. *Adv. Mater.* **2012**, *24* (29), 3975–3980.
- (4) (a) Hoogenboom, R. *Angew. Chemie - Int. Ed.* **2010**, *49* (20), 3415–3417. (b) Massi, A.; Nanni, D. *Org. Biomol. Chem.* **2012**, *10* (19), 3791–3807. (c) Lowe, A. B. *Polym. (United Kingdom)* **2014**, *55* (22), 5517–5549.
- (5) (a) Dondoni, A. *Angew. Chemie - Int. Ed.* **2008**, *47* (47), 8995–8997. (b) Hoyle, C. E.; Lowe, A. B.; Bowman, C. N. *Chem. Soc. Rev.* **2010**, *39* (4), 1355. (c) Hoyle, C. E.; Bowman, C. N. *Angew. Chemie - Int. Ed.* **2010**, *49* (9), 1540–1573. (d) Chan, J. W.; Hoyle, C. E.; Lowe, A. B. *J. Am. Chem. Soc.* **2009**, *131*, 5751–5753. (e) Dondoni, A.; Marra, A. *Chem. Soc. Rev.* **2012**, *41* (2), 573–586. (f) Lowe, A. B. *Polym. Chem.* **2014**, *5* (17), 4820. (g) Fairbanks, B. D.; Love, D. M.; Bowman, C. N. *Macromol. Chem. Phys.* **2017**, *201700073*, 1700073.
- (6) (a) Grim, J. C.; Marozas, I. A.; Anseth, K. S. *J. Control. Release* **2015**, *219*, 95–106. (b) Wang, Y.; Chou, D. H. C. *Angew. Chemie - Int. Ed.* **2015**, *54* (37), 10931–10934. (c) Bañuls, M. J.; Jiménez-Meneses, P.; Meyer, A.; Vasseur, J. J.; Morvan, F.; Escorihuela, J.; Puchades, R.; Maquieira, Á. *Bioconjug. Chem.* **2017**, *28* (2), 496–506.
- (7) (a) Shih, H.; Fraser, A. K.; Lin, C. C. *ACS Appl. Mater. Interfaces* **2013**, *5* (5), 1673–1680. (b) Anderson, S. B.; Lin, C. C.; Kuntzler, D. V.; Anseth, K. S. *Biomaterials* **2011**, *32* (14), 3564–3574. (c) Schwartz, M. P.; Fairbanks, B. D.; Rogers, R. E.; Rangarajan, R.; Zaman, M. H.; Anseth, K. S. *Integr. Biol.* **2010**, *2* (1), 32–40. (d) Polizzotti, B. D.;

- 1  
2  
3 Fairbanks, B. D.; Anseth, K. S. *Biomacromolecules* **2008**, *9* (4), 1084–1087.
- 4  
5 (8) (a) Carioscia, J. A.; Stansbury, J. W.; Bowman, C. N. *Polymer (Guildf)*. **2007**, *48* (6), 1526–1532. (b) Shin, J.;  
6 Matsushima, H.; Comer, C. M.; Bowman, C. N.; Hoyle, C. E. *Chem. Mater.* **2010**, *22* (8), 2616–2625. (c) Chan, J. W.;  
7 Hoyle, C. E.; Lowe, A. B. *J. Am. Chem. Soc.* **2009**, *131* (16), 5751–5753. (d) Uysal, B. B.; Gunay, U. S.; Hizal, G.;  
8 Tunca, U. *J. Polym. Sci. Part A Polym. Chem.* **2014**, *52* (11), 1581–1587. (e) Yu, L.; Wang, L.-H.; Hu, Z.-T.; You, Y.-  
9 Z.; Wu, D.-C.; Hong, C.-Y. *Polym. Chem.* **2015**, *6* (9), 1527–1532. (f) Xi, W.; Pattanayak, S.; Wang, C.; Fairbanks, B.;  
10 Gong, T.; Wagner, J.; Kloxin, C. J.; Bowman, C. N. *Angew. Chemie - Int. Ed.* **2015**, *54* (48), 14462–14467.
- 11  
12  
13  
14  
15 (9) Colak, B.; Da Silva, J. C. S.; Soares, T. A.; Gautrot, J. E. *Bioconjug. Chem.* **2016**, *27* (9), 2111–2123.
- 16  
17 (10) Bernasconi, C. F.; Killion, R. B. *J. Am. Chem. Soc.* **1988**, *110* (22), 7506–7512.
- 18  
19 (11) Irving, R. J.; Nelander, L.; Wadsö, I. *Acta Chemica Scandinavica*. 1964, pp 769–787.
- 20  
21 (12) Kaupmees, K.; Trummal, A.; Leito, I. *Croat. Chem. Acta* **2014**, *87* (4), 385–395.
- 22  
23 (13) Perrin, D. D.; Dempsey, B.; Serjeant, E. P. *pK<sub>a</sub> Prediction for Organic Acids and Bases*; 1981; Vol. 52.
- 24  
25 (14) Leonard, B. Y. **1957**, *151* (6), 1954–1956.
- 26  
27 (15) Gross, K. C.; Seybold, P. G. *Int. J. Quantum Chem.* **2000**, *80* (March), 1107–1115.
- 28  
29 (16) (a) Fairbanks, B. D.; Scott, T. F.; Kloxin, C. J.; Anseth, K. S.; Bowman, C. N. *Macromolecules* **2009**, *42*, 211–217. (b)  
30 Fairbanks, B. D.; Sims, E. A.; Anseth, K. S.; Bowman, C. N. *Macromolecules* **2010**, *43* (9), 4113–4119.
- 31  
32 (17) Cramer, N. B.; Reddy, S. K.; O'Brien, A. K.; Bowman, C. N. *Macromolecules* **2003**, *36* (21), 7964–7969.
- 33  
34 (18) Cramer, N. B.; Davies, T.; Brien, A. K. O.; Bowman, C. N. *Macromolecules* **2003**, *36*, 4631–4636.
- 35  
36 (19) (a) Lawrence, C. C.; Bennati, M.; Obias, H. V.; Bar, G.; Griffin, R. G.; Stubbe, J. *Proc. Natl. Acad. Sci. U. S. A.* **1999**, *96*  
37 (16), 8979–8984. (b) Zipse, H.; All. *J. Org. Chem* **2008**, *131*, 200–211. (c) Chatgililoglu, C.; Asumus, K.-D. *Sulfur-*  
38 *Centered Reactive Intermediates in Chemistry and Biology*, 1st ed.; Chatgililoglu, C., Asumus, K.-D., Eds.; Plenum  
39 Press: New York, 1990. (d) Starke, D. W.; Chock, P. B.; Mieyal, J. J. *J. Biol. Chem.* **2003**, *278* (17), 14607–14613. (e)  
40 Nagy, P. *Antioxid. Redox Signal.* **2013**, *18*, 1623–1641.
- 41  
42  
43 (20) (a) Antonello, S.; Benassi, R.; Gavioli, G.; Taddei, F.; Maran, F. *J. Am. Chem. Soc.* **2002**, *124* (25), 7529–7538. (b)  
44 Antonello, S.; Daasbjerg, K.; Jensen, H.; Taddei, F.; Maran, F. *J. Am. Chem. Soc.* **2003**, *125* (48), 14905–14916. (c)  
45 Yamaji, M.; Tojo, S.; Takehira, K.; Tobita, S.; Fujitsuka, M.; Majima, T. *J. Phys. Chem. A* **2006**, *110* (50), 13487–  
46 13491.
- 47  
48  
49 (21) Hansch, C.; Leo, a; Taft, R. W. *Chem. Rev.* **1991**, *91* (2), 165–195.
- 50  
51 (22) Degirmenci, I.; Coote, M. L. *J. Phys. Chem. A* **2016**, *120* (37), 7398–7403.
- 52  
53 (23) Gobl, M.; Bonifacic, M.; Asmus, K.-D. *J. Am. Chem. Soc.* **1984**, *106* (20), 5984–5988.
- 54  
55 (24) (a) Pauling, L. *J. Am. Chem. Soc.* **1931**, *53* (9), 3225–3237. (b) Clark, T. *ChemPhysChem* **2017**, *1*–7.
- 56  
57  
58  
59  
60

- 1  
2  
3 (25) (a) Exner, O.; Böhm, S. *New J. Chem.* **2008**, 32 (8), 1449. (b) Karni, M.; Bernasconi, C. F.; Rappoport, Z. *J. Org. Chem.*  
4 **2008**, 73 (8), 2980–2994.  
5  
6 (26) (a) Saveant, J. M. *J. Am. Chem. Soc.* **1987**, 109 (c), 6788–6795. (b) Savéant, J.-M. *Electron transfer, bond breaking and*  
7 *bond formation*; 2000; Vol. 35.  
8  
9 (27) Antonello, S.; Benassi, R.; Gavioli, G.; Taddei, F.; Maran, F. *J. Am. Chem. Soc.* **2002**, 124, 7529–7538.  
10  
11 (28) Matyushov, D. V. *Chem. Phys.* **1996**, 211 (1–3), 47–71.  
12  
13 (29) Sumi, H.; Marcus, R. A. *J. Chem. Phys.* **1986**, 84 (9), 4894–4914.  
14  
15 (30) (a) Dumont, É.; Laurent, A. D.; Assfeld, X.; Jacquemin, D. *Chem. Phys. Lett.* **2011**, 501 (4–6), 245–251. (b) Dupont, C.;  
16 Dumont, É.; Jacquemin, D. *J. Phys. Chem. A* **2012**, 116 (12), 3237–3246. (c) Vydrov, O. A.; Scuseria, G. E. *J. Chem.*  
17 *Phys.* **2006**, 125 (23). (d) Dunning Jr, T. H. *J. Chem. Phys.* **1989**, 90 (1989), 1007. (e) Hariharan, P. C.; Pople, J. A.  
18 *Theor. Chim. Acta* **1973**, 28 (3), 213–222. (f) Denis, P. A. *J. Chem. Theory Comput.* **2005**, 1, 900–907.  
19  
20 (31) Li, H.; Jensen, J. H. *J. Comput. Chem.* **2004**, 25 (12), 1449–1462.  
21  
22 (32) Gaussian, Inc.: Wallingford CT 2016.  
23  
24 (33) Tanaka, R.; Yamashita, M.; Chung, L. W.; Morokuma, K.; Nozaki, K. *Organometallics* **2011**, 30 (24), 6742–6750.  
25  
26 (34) (a) De Proft, F.; Martin, J. M. L.; Geerlings, P. *Chem. Phys. Lett.* **1996**, 250 (3–4), 393–401. (b) Cioslowski, J. *J. Am.*  
27 *Chem. Soc.* **1989**, 111 (22), 8333–8336.  
28  
29 (35) (a) Cossi, M.; Barone, V. *J. Chem. Phys.* **2000**, 112 (2000), 2427. (b) Cossi, M.; Barone, V. *J. Phys. Chem. A* **2000**, 104,  
30 10614–10622.  
31  
32 (36) Becke, A. D. *J. Chem. Phys.* **1993**, 98 (7), 5648.  
33  
34 (37) Jursic, B. S. *Int. J. Quantum Chem.* **1997**, 62 (3), 291–296.  
35  
36 (38) Qiu, J.; Zhao, Y.; Li, Z.; Wang, H.; Fan, M.; Wang, J. *ChemSusChem* **2017**, 10 (6), 1120–1127.  
37  
38 (39) Paliwal, P. K.; Jetti, S. R.; Jain, S. *Med. Chem. Res.* **2013**, 22 (6), 2984–2990.  
39  
40  
41  
42  
43  
44  
45  
46  
47  
48  
49  
50  
51  
52  
53  
54  
55  
56  
57  
58  
59  
60